Formation of Persistent Hyperplastic Primary Vitreous in Ephrin-A5$^{-/-}$ Mice

Alexander I. Son,[1] Michal Sheleg,[1] Margaret A. Cooper,[2] Yuhai Sun,[1] Norman J. Kleiman,[3] and Renping Zhou[1]

[1]Department of Chemical Biology, Susan Lehman-Cullman Laboratory for Cancer Research, Ernest Mario School of Pharmacy, Rutgers University, Piscataway, New Jersey
[2]Department of Molecular Biophysics and Biochemistry, Yale University, New Haven, Connecticut
[3]Department of Environmental Health Sciences, Mailman School of Public Health, Columbia University, New York, New York

Correspondence: Renping Zhou, Department of Chemical Biology, Susan Lehman-Cullman Laboratory for Cancer Research, Ernest Mario School of Pharmacy, Rutgers University, Piscataway, NJ 08854; rzhou@rci.rutgers.edu.

Submitted: June 30, 2013
Accepted: February 7, 2014

Citation: Son AI, Sheleg M, Cooper MA, Sun Y, Kleiman NJ, Zhou R. Formation of persistent hyperplastic primary vitreous in ephrin-A5$^{-/-}$ mice. *Invest Ophthalmol Vis Sci.* 2014;55:1594–1606. DOI:10.1167/iovs.13-12706

Purpose. Primary vitreous regression is a critical event in mammalian eye development required for proper ocular maturity and unhindered vision. Failure of this event results in the eye disease persistent hyperplastic primary vitreous (PHPV), also identified as persistent fetal vasculature (PFV), a condition characterized by the presence of a fibrovascular mass adjacent to the lens and retina, and associated with visual disability and blindness. Here, we identify ephrin-A5 to be a critical regulator for primary vitreous regression.

Methods. Wild-type and ephrin-A5$^{-/-}$ eyes were examined at various developmental stages to determine the progression of PHPV. Eye tissue was sectioned and examined by H&E staining. Protein expression and localization was determined through immunohistochemistry. Relative levels of Eph receptors were determined by RT-PCR.

Results. Ephrin-A5$^{-/-}$ animals develop ocular phenotypes representative of PHPV, most notably the presence of a large hyperplastic mass posterior to the lens that remains throughout the lifetime of the animal. The aberrant tissue in these mutant mice consists of residual hyaloid vessels surrounded by pigmented cells of neural crest origin. Labeling with bromodeoxyuridine (BrdU) and detection of proliferating cell nuclear antigen (PCNA) expression shows that the mass in ephrin-A5$^{-/-}$ animals is mitotically active in embryonic and postnatal stages.

Conclusions. Ephrin-A5 is a critical factor that regulates primary vitreous regression.

Keywords: ephrin, Eph receptor, primary vitreous, persistent hyperplastic primary vitreous, persistent fetal vasculature

The primary vitreous is a transient collection of cells encompassing the vitreous humor in the early stages of ocular development. Composed of cells originating from the neural crest and mesoderm,[1,2] this structure eventually gives rise to the hyaloid vasculature, which provides nutrients to the early eye tissues.[3–5] While important in the early formative periods of eye development, the regression of the structures derived from the primary vitreous is a critical event important for the formation of the crystalline vitreous, allowing for light to travel unimpeded to the retina and ensuring proper vision.

Failed regression of the primary vitreous has severe consequences, the most prominent resulting in the eye disease persistent hyperplastic primary vitreous (PHPV), more recently named as persistent fetal vasculature (PFV).[4,6,7] The PHPV and PHPV-like conditions are characterized by the presence of an aberrant retrolental mass consisting of fibrovascular tissue and, in some instances, surrounded by pigmented tissue.[4,6–12] This disease often is classified into an anterior form, posterior form, or combination of both depending on whether the uncharacteristic vascular mass extends from the back of the lens or attaches to the retina, respectively.[4,7] The human form of this disorder often occurs unilaterally, although bilateral cases have been reported previously.[7,12] In addition, PHPV often is associated with other ophthalmologic disorders, including microphthalmia, retinal folding, intraocular hemorrhage, and cataracts.[6,7] This disorder also has been reported prominently in other mammalian species, most notably in several breeds of dogs.[8,13–15] Previous studies have revealed several genetic and cellular factors that contribute to the primary vitreous regression, using transgenic mouse models that develop PHPV-like phenotypes. These include knock-out models for the Arf tumor suppressor gene,[16–19] p53,[20] and Frizzled-5,[21] along with an overexpression model for VEGF.[22,23] However, the molecular and cellular mechanisms underlying formation of PHPV remain under-studied.

In the current study, we have identified a ligand of the Eph family of receptor tyrosine kinases, ephrin-A5, to be critical in the regression of the primary vitreous. The Eph receptors are the largest group of receptor tyrosine kinases; in mammals, this family consists of 14 receptors, divided into the EphA and EphB subgroups, and eight ligands, segregated into the ephrin-A and ephrin-B types.[24] Binding between ligand–receptor pairs occurs promiscuously, with EphA receptors primarily binding to most ephrin-A ligands, while EphB receptors interact with most ephrin-B ligands with certain exceptions, such as interactions between the A-class ligand ephrin-A5 and the B-class receptor EphB2.[25,26] Ephrin ligands are bound to the cell surface, with the ephrin-As attached by a glycosylphosphati-

dylinositol (GPI) anchor and the ephrin-Bs having a short transmembrane segment. Receptor activation by membrane-bound ligands allows for signals to the receptor-expressing cell (forward signaling), ligand-expressing cell (reverse signaling), or bidirectional signaling.[27–29] The GPI-anchored ephrin-As also have the capacity to be cleaved,[30] and soluble ephrin-As in monomeric and oligomeric forms have been found to regulate Eph receptor signaling in vitro.[31,32]

The Eph receptor family has been implicated in diverse biological and developmental processes, including neural development, blood vessel formation, and cancer.[26] Additionally, the Eph family has key roles in ocular development, with several Eph receptors and ligands expressed in the eye.[33–35] We and others have shown that the ligand ephrin-A5 has multiple functions in the nervous system[36–40] and lens development.[33,34,41–43] Here, we reported that mice lacking ephrin-A5 also develop characteristics indicative of PHPV, including the presence of a hyperplastic mass consisting of pigmented and vascular cells posterior to the lens. In addition, we showed that in these mice, the retrolental cell mass develops not because of the failure of hyaloid vessel regression, but rather due to abnormal recruitment of cells into the primary vitreous during early eye development, implicating a new mechanism of PHPV pathogenesis. Our observations suggested a critical role of ephrin-A5 in regulating proper cell migration into the primary vitreous during early eye morphogenesis.

Materials and Methods

Animal Care

Mice were bred and maintained under standard conditions in accordance with the Guidelines for the Care and Use of Laboratory Animals of Rutgers University and the ARVO Statement for the Use of Animals in Ophthalmic and Vision Research. Ephrin-A5$^{-/-}$ mice have been described previously,[44] and are under a mixed background of S129 and C57BL/6 strains.

Hematoxylin and Eosin Staining

Hematoxylin and eosin (H&E) staining protocols have been described previously.[33] Briefly, embryo heads (embryonic day 14 [E14], E17, and P0) or dissected eyes (postnatal day 6 [P6], P21, and P60) were prepared in fixation buffer (65% ethanol, 4% formaldehyde, 5% acetic acid, 3% sucrose) at 4°C overnight, dehydrated the following day, and embedded in Paraplast (McCormick Scientific, St. Louis, MO). Longitudinal sections were prepared at 5 μm and stained with H&E (Sigma-Aldrich, St. Louis, MO).

Immunohistochemistry

Adult wild-type and ephrin-A5$^{-/-}$ eyes were enucleated and fixed in 4% formaldehyde for 10 minutes at room temperature, followed by a rinse in PBS for 5 minutes, and stored in 10% sucrose overnight at 4°C. Embryonic tissue was fixed in 4% paraformaldehyde for 60 minutes at room temperature, followed by three rinses in PBS for 10 minutes each, and stored in 30% sucrose overnight at 4°C. All tissues subsequently were frozen and cryosectioned at 10 μm.

Primary vitreous structures were observed using various antibodies. Neural crest cells were identified using anti-AP2β antibody (1:200, Cat. #2509; Cell Signaling Technology, Inc., Danvers, MA). Mesenchymal and endothelial cells were determined using antibodies against CD-31 (1:200, Cat. #550244; BD Biosciences, San Jose, CA) and the vascular basal membrane marker collagen-IV (1:200, Cat. #2150-1470; AbD Serotec, Kidlington, UK), respectively. Perivascular smooth muscle cells were identified using an antibody against α-smooth muscle actin (1:200, Cat. #A 2547; Sigma-Aldrich). Pericytes were identified using an antibody against platelet-derived growth factor-β (PDGFRβ; 1:200, Cat. #14-1402; eBioscience, Inc., San Diego, CA). Macrophages were identified using antibodies against F4/80 (1:200, Cat. #MF48000; Invitrogen, Carlsbad, CA) and ED-1 (1:200, Cat. #Ab31630; Abcam, Cambridge, UK). Pigmented cells were stained using an antibody against tyrosinase related protein (TRP)-1 (1:200, Cat. #sc-10448; Santa Cruz Biotechnology, Inc., Santa Cruz, CA). EphA2 receptor localization was determined using antibodies against EphA2 (1:200, Cat. #AF639; R&D Systems, Minneapolis, MN). Primary antibodies were incubated overnight at 4°C and washed in PBS, followed by detection using goat or donkey secondary antibodies conjugated with Alexa Fluor 488 (Invitrogen) or CY3 (Jackson ImmunoResearch Laboratories, Inc., West Grove, PA) at room temperature for 2 hours. Nuclei were stained using TO-PRO-3 iodide far red fluorescence dye (1:1000, Cat. #T3605; Invitrogen).

To determine Eph receptor localization using ephrin-A5-Fc, adult eyes were enucleated, fixed, and sectioned as described earlier. Tissue was treated with ephrin-A5-Fc fusion protein (Cat. #374-EA-200; R&D Systems) at 10 μg/mL overnight at 4°C and washed in PBS, and labeling detected using a biotin-conjugated goat anti-human antibody (1:200; Jackson ImmunoResearch Laboratories, Inc.) followed by CY3-conjugated streptavidin (1:1000; Jackson ImmunoResearch Laboratories, Inc.).

Cell division was determined through bromodeoxyuridine (BrdU) treatment and detection, and proliferating cell nuclear antigen (PCNA) labeling. Bromodeoxyuridine (Cat. #B5002; Sigma-Aldrich) was dissolved in a 0.007 Normal (N) NaOH solution made in 0.9% NaCl at 5 mg/mL and injected intraperitoneally at a concentration of 50 μg/g body weight. Eye tissue was fixed and sectioned as described previously. Sections were treated in 2 N HCl at 37°C for 30 minutes, followed by a rinse in 0.1 M sodium borate, pH 8.5, at room temperature for 10 minutes. The BrdU incorporation was detected using an antibody against BrdU (1:100, Cat. #OBT0030G; Accurate Chemical & Scientific Corporation, Westbury, NY). Cell division also was determined using an antibody against PCNA (1:100, Cat. #sc-25280; Santa Cruz Biotechnology, Inc.). Before staining, slides were boiled in 0.1 M citrate buffer for 10 minutes and cooled at room temperature in the same buffer for 20 minutes. Slides then were immersed in 3% hydrogen peroxide solution in PBS for 10 minutes. Apoptosis was determined using an antibody against cleaved caspase-3 (1:200, #9661; Cell Signaling Technology, Inc.).

Whole Mount Hyaloid Preparation

Wild-type and ephrin-A5$^{-/-}$ eyes at P2, P8, P14, P21, and P40 were enucleated and their corneas removed. The dissected eyes were fixed overnight in 4% paraformaldehyde, after which the eyes were rinsed in PBS. The retinal cup along with the lens then was removed from the sclera carefully, after which the retina was dissected apart from the posterior pole with the hyaloid vessels still intact and attached to the lens. Lenses with the hyaloid network were stained in FITC-conjugated isolectin-B4 overnight (1:500, Cat. #FL-1201; Vector Laboratories, Burlingame, CA), rinsed in PBS, and mounted in Clear Mount Medium (17985-16; Electron Microscopy Sciences, Hatfield, PA). The Z-stack images were taken using a Nikon Eclipse C1 confocal microscope system. Quantification of vessels from the tunica vasculosa lentis (TVL) have been described previously.[3] Briefly, a circle with a radius 70.7% of the lens was drawn on

Investigative Ophthalmology & Visual Science

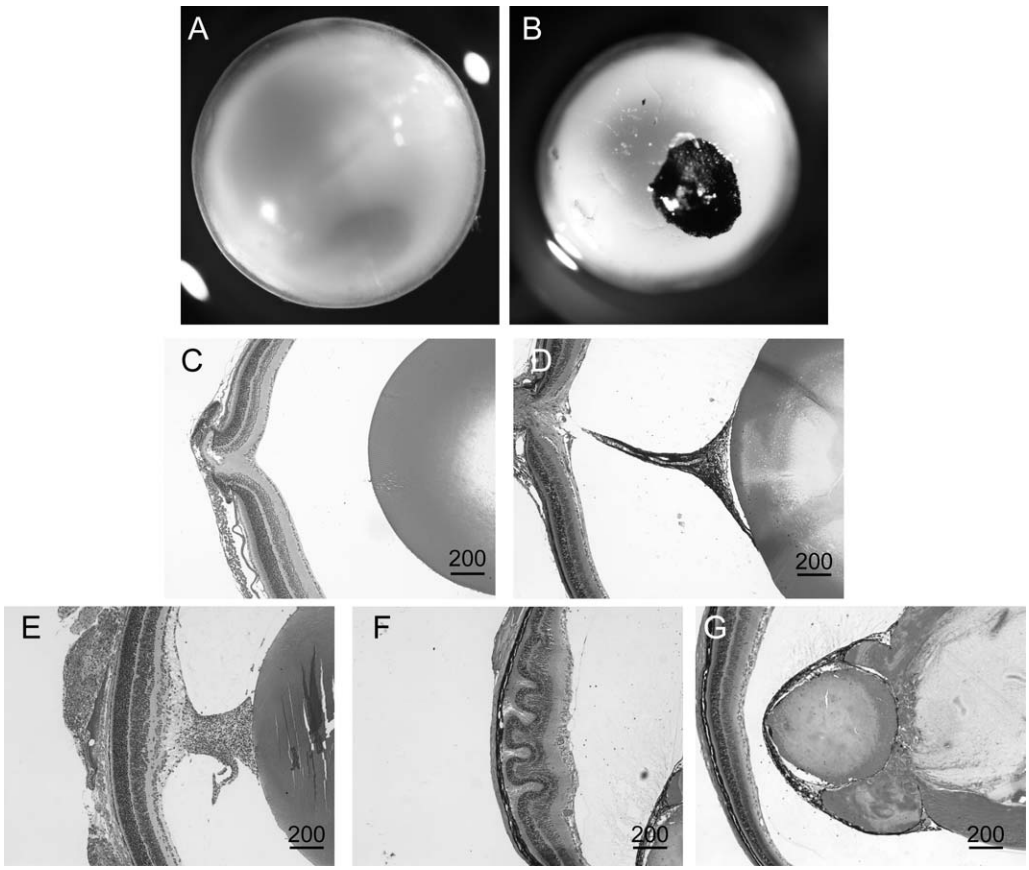

Figure 1. Ephrin-A5$^{-/-}$ mice develop hallmark symptoms of PHPV. (**A**, **B**) Whole mount lenses from P21 wild-type (**A**) and ephrin-A5$^{-/-}$ (**B**) eyes. Ephrin-A5$^{-/-}$ eyes display the presence of a thick pigmented mass adjacent to the posterior lens. (**C**, **D**) Histologic sections of wild-type and ephrin-A5$^{-/-}$ eyes at P21. (**E**–**G**) Adult Ephrin-A5 mutant eyes display other symptomatic characteristics of PHPV. These include tissue attachment to the retina and lens (**E**), retinal folding and detachment of the RPE layer from the neuroretina (**F**), and lens capsule rupture (**G**). *Scale bars* in μm.

the posterior lens (equivalent to the 45° latitudinal line), and vessels crossing this line were counted.

Real Time RT-PCR

Ephrin-A5$^{-/-}$ eyes were enucleated and the retrolental mass was removed carefully under a dissecting microscope. RNA was extracted from the tissue using the RNeasy Mini Kit (Cat. #74104; Qiagen, Valencia, CA) as per the manufacturer's instructions. The resulting RNA was amplified using the MessageAmp II aRNA Amplification Kit (Cat. #AM1751; Ambion, Inc., Austin, TX). Reverse transcription of the resulting RNA into cDNA was performed using SuperScript II Reverse Transcriptase (Cat. #18064-022; Invitrogen, Grand Island, NY) as per the manufacturer's instructions. Primers of the various Eph receptors that were used have been published previously.[45] RNA levels were analyzed using the ABI PRISM 7000 system.

Detection of Ephrins With EphA5-Alkaline Phosphatase Fusion Protein

Three different commercially available ephrin-A5 antibodies (Cat. #70114; Abcam; and Cat. #sc-1951 and Cat. #sc-6075; Santa Cruz Biotechnology, Inc.) were tested for immunohistochemistry; however, none detected ephrin-A5 specifically, since the ephrin-A5$^{-/-}$ control showed similar staining patterns to wild-type tissues. Due to a lack of high quality antibodies against ephrin-A5, we employed EphA5-Alkaline Phosphatase (AP) fusion protein staining for ephrin ligand expression as has been described previously.[46,47] EphA5-AP contains the extracellular domain of EphA5 fused in-frame to alkaline phosphatase, and thus can bind to A-class ephrins. Ephrin ligand binding was determined on frozen tissue sectioned at 14 μm mounted onto slides. Sections were fixed in 4% paraformaldehyde in PBS for 8 minutes at room temperature, followed by two washes in PBS 5 minutes each. Media containing EphA5-AP then was applied to the sections for 2 hours, followed by washes in Hank's balanced salt solution with 0.5 mg/mL BSA and 20 mM HEPES (pH 7.0). Sections were fixed again in 3% formaldehyde and 20 mM HEPES (pH 7.5) for 30 seconds, followed by two washes in Wash Buffer (150 mM NaCl and 20 mM HEPES [pH 7.5]) for 5 minutes each. Sections then were heated to 65°C for 15 minutes and washed again in Wash Buffer, followed by a rinse in AP Color Development Buffer (100 mM Tris-HCl [pH. 9.5], 100 mM NaCl, 5 mM $MgCl_2$). Color development was done by adding AP Color Development Buffer with NBT/BCIP solution and incubated at room temperature until sections were stained sufficiently.

Quantifications and Volumetric Analysis of Retrolental Mass

To quantify primary vitreous cells within wild-type and ephrin-A5$^{-/-}$ animals, embryos were cryosectioned at 10 μm with sections collected in series, stained, and analyzed. Only cells within the vitreous space were counted. To analyze the volume of the retrolental mass in postnatal animals, frozen sections

Investigative Ophthalmology & Visual Science

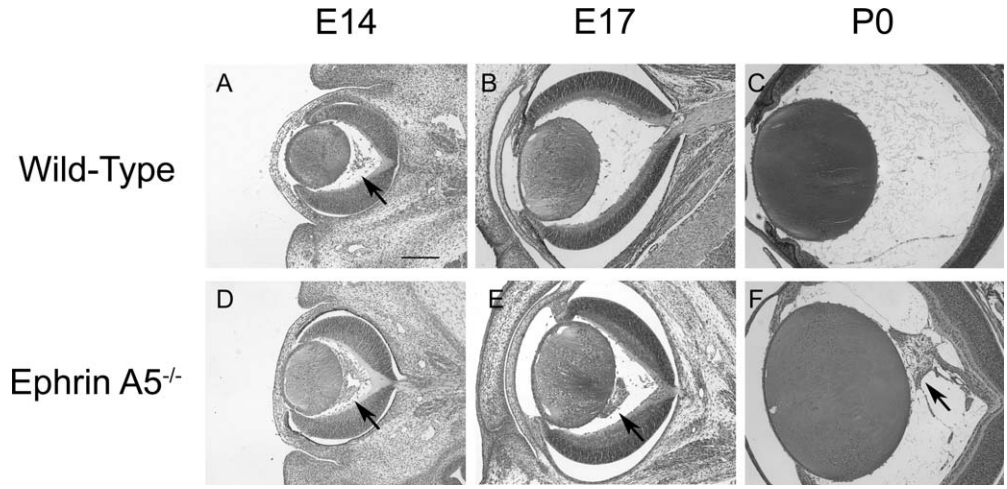

Figure 2. Persistent retrolental mass originates from the primary vitreous at embryonic stages. (**A–F**) Sections of wild-type (**A–C**) and ephrin-A5$^{-/-}$ (**D–F**) eyes during embryonic development. The cells of the primary vitreous are present in the wild-type eye at E14 ([**A**], as indicated by the *arrows*), but soon regress and are absent at later developmental stages (**B**, **C**). In contrast, primary vitreous cells in the ephrin-A5$^{-/-}$ eye that appear in early embryogenesis (**D**) fail to regress (**E**, **F**). *Scale bar*: 200 μm.

were collected at 10 μm containing the mass at either P7 or P21 and stained with an antibody against TRP-1. The areas of each section then were calculated using ImageJ (available in the public domain at http://rsbweb.nih.gov/ij/) and multiplied by the thickness of each section.

Results

Ephrin-A5$^{-/-}$ Mice Develop Symptoms Indicative of PHPV

Previous studies by our group and others have shown that ephrin-A5$^{-/-}$ animals develop cataracts.[33,41,42] As a result, we asked whether other ocular anomalies were present in the ephrin-A5 mutant eye (Fig. 1). While wild-type eyes exhibited no abnormalities (Figs. 1A, 1C), whole-mount and histologic investigation of postnatal ephrin-A5$^{-/-}$ eyes revealed the presence of a large pigmented mass encapsulating vasculature posterior to the lens and extending toward the retina in a funnel-like shape, indicative of the pathology of PHPV (Figs. 1B, 1D). In addition to the attachment of the hyperplastic mass to the neuroretina and the posterior of the lens (Fig. 1E), ephrin-A5$^{-/-}$ eyes exhibited several additional hallmark characteristics of PHPV, including retinal folding, neuroretinal detachment from the RPE layer, and lens capsule rupture in later ages (Figs. 1F, 1G). These phenotypes were found in approximately half of the adult mutant eyes older than 2 months, specifically associated with ruptured lens, which presses onto the retina, indicating that these phenotypes are secondary to lens damage as reported previously.[33,43]

We further examined the progression of the retrolental mass during prenatal eye development to determine the origin of this mass (Fig. 2). In wild-type eyes, the retrolental primary vitreous cell mass was present at E14 (Fig. 2A), but was noticeably regressed by E17 and absent by birth (Figs. 2B, 2C). No wild type animals past P0 showed signs of the retrolental primary vitreous cell mass (see Figs. 1A, 1C, 2C). The retrolental cell mass also is present in ephrin-A5$^{-/-}$ eyes at E14 (Fig. 2D); however, the mass in these animals fails to regress during prenatal stages and persists postnatally (Figs. 2E, 2F). When analyzing the prevalence of PHPV, almost all adult wild-type mice (>P60) displayed no presence of a retrolental mass, while all ephrin-A5$^{-/-}$ animals and approximately half of the ephrin-A5$^{+/-}$ subjects were observed to have the presence of an abnormal retrolental mass with vasculature and pigmented cells (wild-type = 1.8%, ephrin-A5$^{-/-}$ = 100%, ephrin-A5$^{+/-}$ = 49.2%; see Table).

Vascular Structures Are Present Within the Hyperplastic Mass in the Ephrin-A5$^{-/-}$ Eye

It has been hypothesized that PHPV is the result of the failed regression of the hyaloid vascular system.[4,6,7] We, therefore, analyzed the aberrant structures for vascular markers in the postnatal ephrin-A5$^{-/-}$ eyes (Supplementary Fig. S1). The presence of blood vessels was confirmed through immunofluo-

Table. Prevalence of PHPV

	Wild-Type			Ephrin-A5$^{-/-}$			Ephrin-A5$^{+/-}$		
Age	# With Mass	# Animals	Prevalence	# With Mass	# Animals	Prevalence	# With Mass	# Animals	Prevalence
P0–P5	3	17	17.6%	17	17	100.0%	8	19	42.1%
P6–P10	3	18	16.7%	20	22	90.9%	8	20	40.0%
P21	0	29	0.0%	35	36	97.2%	18	30	60.0%
>P60	1	55	1.8%	55	55	100.0%	30	61	49.2%

Few wild-type animals show the presence of a retrolental mass at early postnatal ages, while almost none are observed in adulthood. In contrast, almost all ephrin-A5$^{-/-}$ animals were found to have an aberrant retrolental mass well into adulthood. Half of the ephrin-A5$^{+/-}$ eyes examined also have an abnormal mass posterior to the lens.

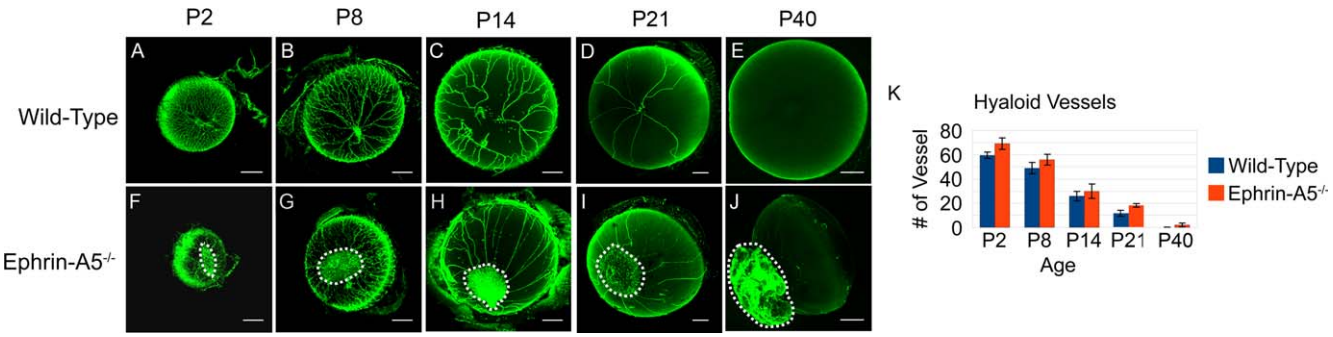

Figure 3. The TVL regression occurs within the ephrin-A5$^{-/-}$ eye. (**A–J**) Whole-mount preparations of lenses viewed from the posterior of wild-type (**A–E**) and ephrin-A5$^{-/-}$ (**F–J**) eyes at several postnatal stages. Lenses are dissected with hyaloid vessels intact and are stained with FITC-conjugated isolectin-B4. Note the presence of the retrolental mass in the ephrin-A5$^{-/-}$ lenses (outlined by a *white dotted line*). *Scale bars*: 0.5 mm. (**K**) Quantification of vessel numbers of the TVL vessels present at several postnatal stages in WT and ephrin-A5$^{-/-}$ mice. Consistent hyaloid regression is observed in the wild-type and ephrin-A5$^{-/-}$ eyes.

rescence using several known markers, including CD-31 (Supplementary Fig. S1B) and collagen-IV (Supplementary Fig. S1C) for endothelial cells, α-smooth muscle actin (αSMA, Supplementary Fig. S1D) for mature pericytes, PDGFRβ (Supplementary Fig. S1E) for immature pericytes, and TRP-1 for melanocytes (Supplementary Fig. S1F). At P7, vascular structures within the hyperplastic mass were found to be positive for the indicated blood vessel markers (Supplementary Figs. S1B–E). However, with the exception of TRP-1, the localization of these markers was restricted to only vessels within the mass, suggesting that the majority of the mass is not of vascular origins. Interestingly, PDGFRβ, a marker known to label primarily pericytes, also was observed on the outer layer of the retrolental structure at P7 as well as on the blood vessels. In contrast, TRP-1 staining was observed throughout much of the hyperplastic tissue, indicating that a major population of cells in this mass is composed of pigmented cells (Supplementary Fig. S1F). The presence of endothelial cells and pericyte precursors in ephrin-A5$^{-/-}$ eyes confirmed that the retrolental mass contains, but is not exclusively consisting of, vascular structures.

Hyaloid Vasculature Regression in Areas Outside of the Hyperplastic Mass Occurs Normally in Ephrin-A5$^{-/-}$ Mice

While remnants of vasculature within the retrolental tissue were observed, the roles these vessels play in the persistence of this pigmented tissue remain unknown. Therefore, we examined whether the persistent mass in ephrin-A5$^{-/-}$ mice was a direct result of a failure of hyaloid regression (Fig. 3). Whole-mount postnatal wild-type and ephrin-A5$^{-/-}$ lenses were enucleated with the hyaloid vasculature attached to the posterior of the lens. Vessels were labeled using FITC-conjugated isolectin B4, and Z-stack images of the posterior lens were taken using confocal microscopy. Vessels of the TVL were analyzed as described previously.[3] Postnatal ephrin-A5$^{-/-}$ eyes had slightly more vessels compared to the wild-type controls (Fig. 3). However, the number of vessels in ephrin-

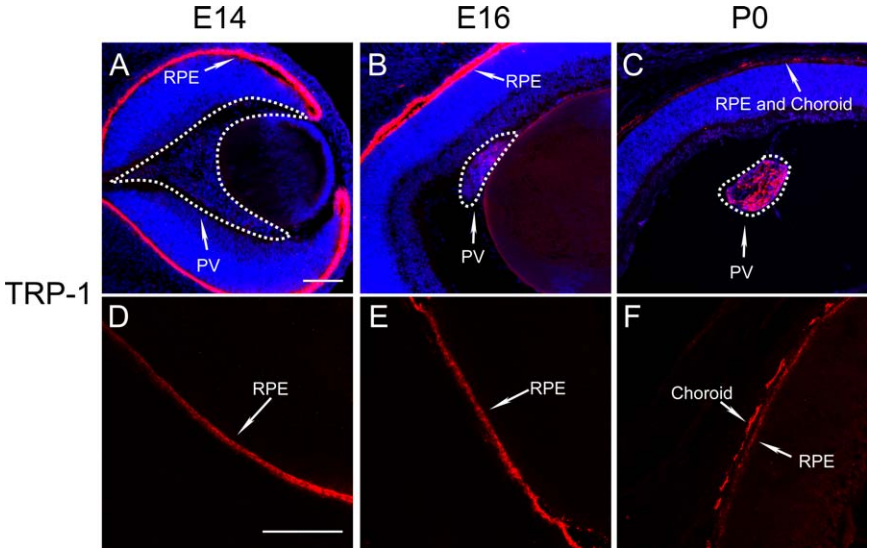

Figure 4. The persistent primary vitreous in the ephrin-A5$^{-/-}$ eye is not pigmented until postnatal stages. (**A–C**) Ephrin-A5$^{-/-}$ eyes stained for TRP-1 at various developmental stages. Cells of the primary vitreous are mostly negative for TRP-1 during prenatal time points E14 and E16 (**A**, **B**). At P0, TRP-1 positive cells are observed clearly in the retrolental mass (**C**). Primary vitreous is outlined by a *white dotted line*. TRP-1 is stained in *red*; nuclear staining is shown in *blue*. PV, primary vitreous. *Scale bar*: 100 μm. (**D–F**) The RPE layer is positive for TRP-1 at embryonic stages. In contrast to the absence of TRP-1 expression in the primary vitreous, the RPE shows positive expression at E14 and later stages (**D**, **E**). Positive expression in the choroid is evident by P0 (**F**). *Scale bar*: 100 μm.

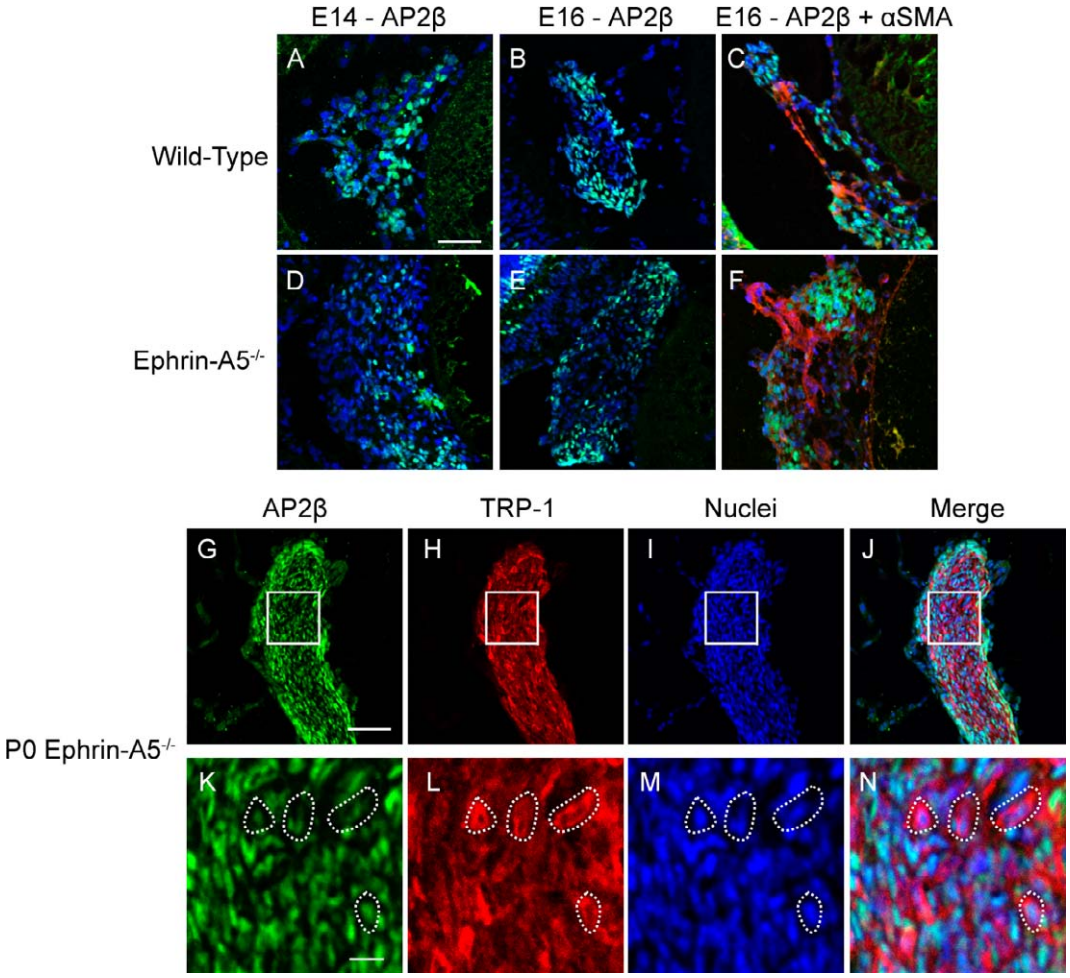

Figure 5. The primary vitreous contains neural crest–derived cells. (**A**, **B**, **D**, **E**) Cells of the primary vitreous stained for neural crest marker AP2β (*green*). Primary vitreous cells at E14 (**A**, **D**) and E16 (**B**, **E**) of wild-type and ephrin-A5$^{-/-}$ tissue are positive for AP2β. (**C**, **F**) Cells of the primary vitreous in wild-type and ephrin-A5$^{-/-}$ embryos show that AP2β+ cells are in a separate population from the vasculature (aSMA+ cells). *Scale bar*: 20 μm. (**G–J**) The persistent primary vitreous in the P0 ephrin-A5$^{-/-}$ eye is positive for AP2β and TRP-1. Pigmented cells, defined by the TRP-1 staining (cytoplasmic), co-label with the AP2β marker (nuclear) indicating cells of neural crest lineage. *Scale bar*: 50 μm. (**K–N**) Higher magnification of the boxed region outlined in (**G–J**), respectively. *Dotted white lines* indicate select cells co-labeled for AP2β and TRP-1. *Scale bar*: 5 μm.

A5$^{-/-}$ eyes consistently decreased over age similar to that of the wild-type controls. Importantly, ephrin-A5$^{-/-}$ eyes at all stages displayed the presence of a distinct retrolental mass (Figs. 3F–J, outlined by white dotted line). Therefore, while the vessels surrounded by the hyperplastic mass persist and do not undergo proper vascular regression, other hyaloid vasculature is able to regress properly in the ephrin-A5$^{-/-}$ eye. Together, these observations suggested that the accumulation of the primary vitreous cell mass, and not hyaloid vessel regression, may be the predominant cause of the pathologic retrolental cellular mass.

Regression of the hyaloid vasculature is regulated in large part by the activity of macrophages.[48] To determine macrophage localization in the context of the retrolental tissue, we labeled cells using the markers F4/80 and ED-1 (Supplementary Fig. S2). The F4/80+ and ED-1+ cells are observed throughout the mass in postnatal stages (Supplementary Figs. S2A, S2B) and also are found within the primary vitreous at embryonic stages in wild-type and ephrin-A5$^{-/-}$ eyes (Supplementary Figs. S2C, S2D). Altogether, the failure of regression of the retrolental cell mass is not due to the absence of macrophages, which have been shown to have a key role in hyaloid vessel regression.[48]

Hyperplastic Mass Exhibits Pigmentation at Postnatal Stages Suggesting a Neural Crest Origin

A characteristic of PHPV and PHPV-like cases is the pigmentation of the retrolental mass.[8–10,12,49,50] Pigmented cells within mammals originate from either the RPE or the neural crest.[51] We observed that the retrolental mass in ephrin-A5$^{-/-}$ animals was pigmented only in postnatal mice (see Figs. 1B, 2D, Supplementary Fig. S1A). To determine the onset of pigmentation within the primary vitreous, we examined the expression profile of the melanin precursor marker TRP-1 in ephrin-A5$^{-/-}$ eyes at various embryonic and postnatal stages (Fig. 4). Expression for TRP-1 was noticeably absent in the primary vitreous during embryogenesis (Figs. 4A, 4B) even though it was present in the RPE layer at these time points (Figs. 4D, 4E). Interestingly, positive TRP-1 labeling was observed in many of the cells within the mass by P0 (Fig. 4C). This rise in expression of TRP-1 in the hyperplastic mass is concurrent with the expression of the marker in the choroid in the postnatal period (Fig. 4F), a tissue of neural crest origin,[52] indicating that the pigmented cells of the primary vitreous forming the retrolental mass in ephrin-A5$^{-/-}$ mice are not from the RPE, but rather from the neural crest.

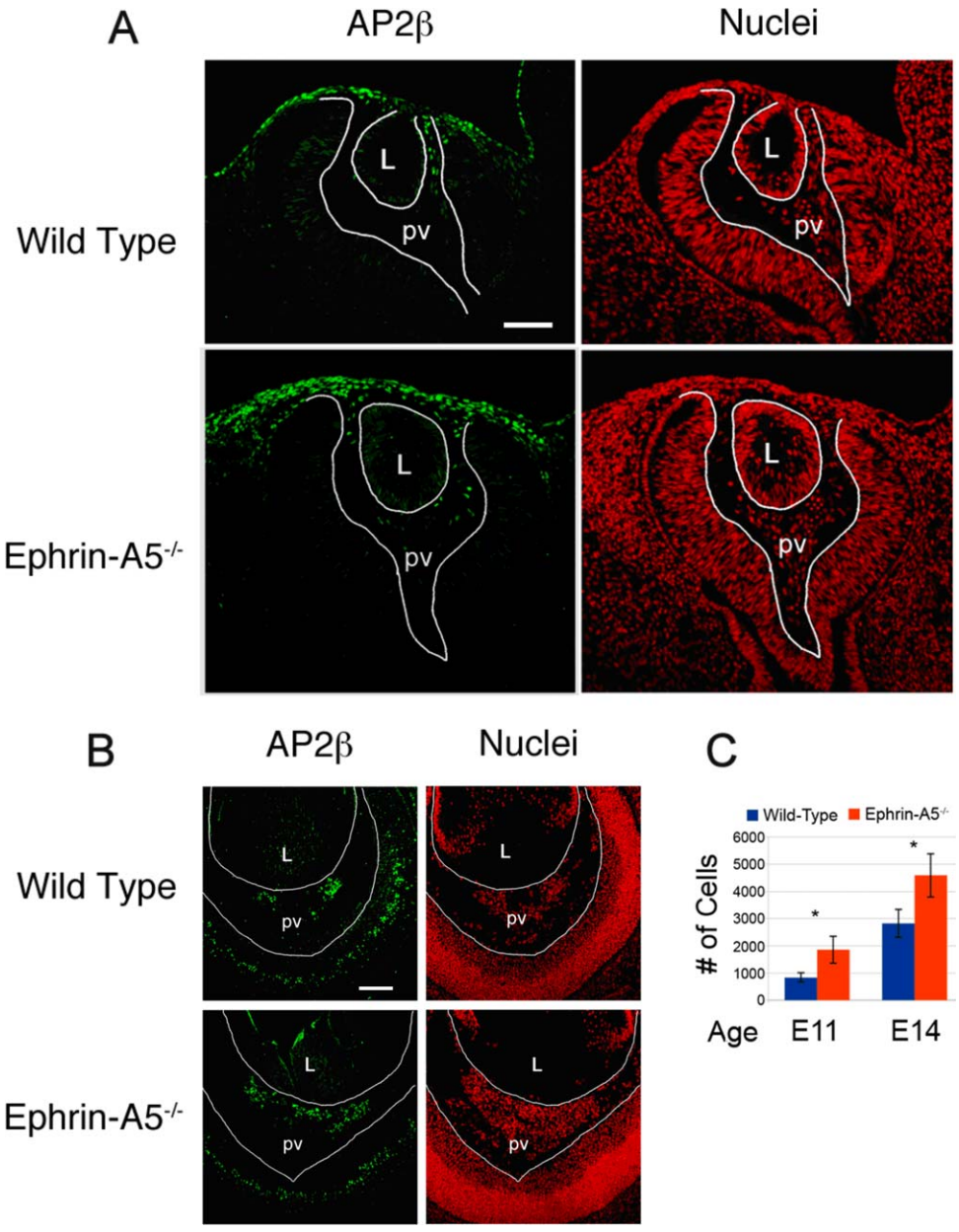

Figure 6. Primary vitreous cells migrate from the corneal region into the vitreous space. (**A**, **B**) AP2β+ (*green*) from the presumptive cornea appear between the lens and retina in wild-type and ephrin-A5$^{-/-}$ eyes at E11 (**A**) and E14 (**B**). Large numbers of CD31-positive mesodermal cells also appear within the retrolental vitreous space at this stage (not shown). L, lens; pv, primary vitreous. *Scale bars*: 100 μm. (**C**) Quantification of the number of cells encompassing the primary vitreous at E11 and E14. While cell numbers increase between E11 and E14 in groups, ephrin-A5$^{-/-}$ eyes consistently show significantly more cells in the primary vitreous ($P < 0.05$, $n = 4$ per group).

To confirm that the persistent primary vitreous cell mass is of neural crest origin, we labeled cells for the transcription factor AP2β, a marker for cells from the neural crest[53] (Fig. 5). Cells expressing AP2β are observed in the retrolental tissue of wild-type and ephrin-A5$^{-/-}$ mice at early developmental stages, including E14 and E16 (Figs. 5A, 5B, 5D, 5E). Cells of this lineage also are distinct from hyaloid vessels, as co-labeling of tissue for AP2β and αSMA shows distinct populations at E16 (Figs. 5C, 5F), revealing that a significant population of cells within the retrolental mass are of neural crest origin. We further established that the persistent retrolental masses in the postnatal ephrin-A5 mutants were of neural crest origin by co-staining P0 ephrin-A5$^{-/-}$ eyes for AP2β and TRP-1 (Figs. 5G–N). Both markers were found throughout the entirety of the hyperplastic mass at this early postnatal stage (Figs. 5G–J). Closer inspection showed that AP2β and TRP-1 labeled the same cells (Figs. 5K–N). These results confirmed previous studies that have shown that the primary vitreous is consisted of neural crest and mesodermal origins.[1,2]

Increased Recruitment of Neural Crest and Mesodermal Cells Into the Primary Vitreous During Early Eye Development in Ephrin-A5$^{-/-}$ Animals

We next set to define the origin of the neural crest cellular population and whether the rate of accumulation of these cells is altered in the ephrin-A5$^{-/-}$ embryos (Fig. 6, Supplementary

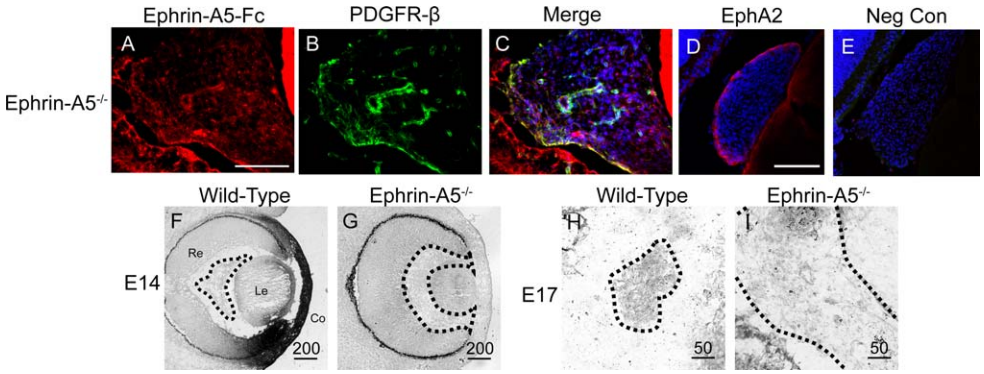

Figure 7. Eph receptor and ephrin-A5 expression within the primary vitreous. (**A–C**) Total Eph receptor localization in the primary vitreous mass. The hyperplastic is labeled with ephrin-A5-Fc to identify Eph receptors capable of binding to the ligand. Eph receptor expression is present throughout much of the mass (**A**) and is not restricted to PDGFR-β+ vasculature (**B**, **C**). Nuclei are counterstained in *blue*. (**D**) Localization of the receptor EphA2 in the retrolental mass. EphA2 expression (*red*) is observed in the outer region of the mass. Nuclei are counterstained in *blue*. (**E**) Negative staining control (no primary antibody) of the retrolental mass in ephrin-A5$^{-/-}$ eyes, with nuclei counterstained in *blue. Scale bars*: 100 μm (**A**, **D**). (**F**, **G**) Ephrin-A5 expression in the E14 eye. EphA5-AP labeling in the developing eye was used to determine ephrin-A ligand expression. Expression is observed at high levels in the cornea, lens, and peripheral tips of the retina in the wild-type (**F**) while absent in the ephrin-A5$^{-/-}$ eye (**G**), indicating ephrin-A5 specificity. However, no labeling is observed in the primary vitreous in either wild-type or ephrin-A5$^{-/-}$ tissues. Primary vitreous is outlined in a *black dotted line*. (**H**, **I**) High magnification images of the primary vitreous at E17 in wild type (**H**) and ephrin-A5$^{-/-}$ (**I**) ocular tissues labeled with EphA5-AP. No strong staining is observed in wild type or ephrin-A5$^{-/-}$ primary vitreous cell mass. Primary vitreous is outlined in a *black dotted line*. Re, retina; Le, lens; Co, Cornea. *Scale bars*: 200 μm (**F**, **G**); 50 μm (**H**, **I**).

Fig. S3). The E11 wild-type and ephrin-A5$^{-/-}$ animals exhibited cells from the neural crest (AP2β) and mesoderm (CD-31) throughout the primary vitreous (data not shown), while the percentage of cells that were AP2β+ or CD31+ cells in the primary vitreous at this stage were similar in genotypes (Supplementary Fig. S3, $P > 0.05$, $n = 4$ per group). Closer inspection near the junction of the cornea, retina, and lens shows neural crest cells to be migrating into the vitreal space from the cornea (Fig. 6A), and these cells appear to collect into the region posterior to the lens to form the primary vitreous (Fig. 6B). In addition, drastically more neural crest cells have been recruited in the E11 and the E14 vitreous (Fig. 6C), suggesting a loss of restriction of cell migration in the developing mutant eye. Together, these data indicated that the pigmented retrolental mass in the postnatal ephrin-A5$^{-/-}$ eye is of neural crest origin, and that there is a loss of restriction of cell recruitment into the developing vitreous.

EphA Receptor Expression Within the Hyperplastic Mass

As ephrin activity is initiated by interactions with their respective Eph receptors, we next set out to examine whether Eph receptors are expressed in the hyperplastic mass (Fig. 7). To determine the localization of Eph receptors in the primary vitreous mass capable of binding to ephrin-A5, we employed a soluble ephrin-A5 protein fused with human-Fc to label Eph receptors in P7 ephrin-A5$^{-/-}$ sections.[54] By using a fluorescent secondary, we observed Eph receptor expression throughout the mass within pigmented cells and the blood vessels (Figs. 7A–C). We also looked for the expression of specific EphA receptors that may be capable of binding with ephrin-A5. EphA2 has been associated previously with neural crest[55] and blood vessel[56–60] development, and has been shown to be activated by ephrin-A5.[33] EphA2 expression was observed within the retrolental mass, but only on the outer edge (Fig. 7D). Examination of mRNA expression using RT-PCR identified several additional EphA receptors, including EphA5, EphA6, and EphA8 (data not shown).

Ephrin-A5 is Expressed at High Levels in the Frontal Eye Segment but Not in the Developing Primary Vitreous

Since the absence of ephrin-A5 results in the failed regression of the primary vitreous, we set to define the expression of the ligand in the developing eye. We had tested several different commercially available ephrin-A5 antibodies and found that none detected ephrin-A5 specifically (data not shown, see Methods and Materials for more details). We, therefore, employed the use of a soluble EphA5 conjugated to alkaline phosphatase (EphA5-AP) to label available ephrins and compared the expression between wild-type and ephrin-A5$^{-/-}$ specimens (Figs. 7F–I). Wild-type and ephrin-A5$^{-/-}$ embryos at E14 and E17 were analyzed, as the normal retrolental tissue still was present at these developmental stages. Strong EphA5-AP staining was observed in the cornea, lens epithelium and bow regions, nasal retina, and ciliary body of wild-type tissue as has been shown previously (Fig. 7F). Little or no positive staining was observed in the ephrin-A5$^{-/-}$ eye (Fig. 7G), indicating that ephrin-A5 is the major A-class ephrin ligand within the developing eye. However, when examining specifically at the primary vitreous, positive AP labeling was notably absent at all stages in wild-type retrolental cell mass (Figs. 7F, 7H), indicating little or no ephrin-A ligand expression in this specific region.

Ephrin-A5$^{-/-}$ Retrolental Cell Mass Continues to Proliferate in Late Embryogenesis and Postnatal Stages

To examine whether the abnormal cell mass is growing in postnatal life, the PHPV tissue sizes at postnatal days 7 and 21 were measured (Fig. 8). A 3-fold increase was observed in these 2-week periods, indicating a continued growth of the abnormal cell mass (Figs. 8A–C). The mitotic activity of the retrolental mass in ephrin-A5$^{-/-}$ eyes continues into postnatal stages, as BrdU incorporation also was observed in P7 ephrin-A5$^{-/-}$ ocular tissues (Fig. 8D). The PCNA expression, another marker for cell division, also was observed in the hyperplastic mass at

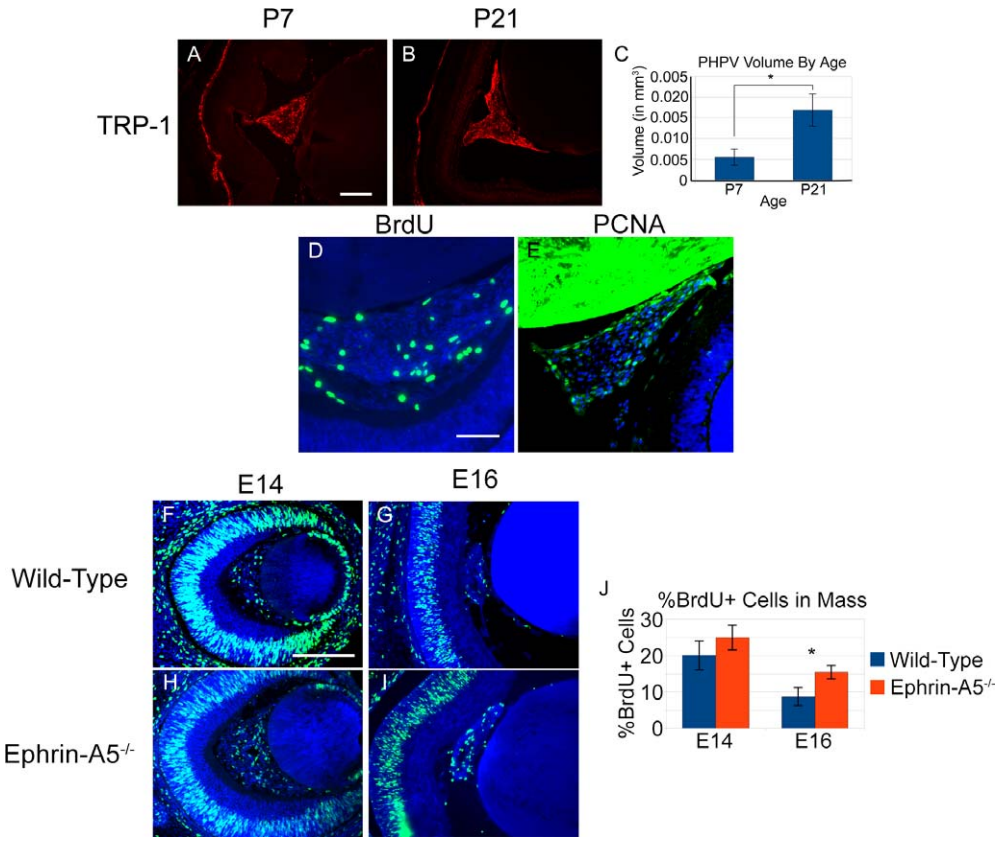

Figure 8. The primary vitreous cell mass continues to grow during late embryogenesis into postnatal stages in the ephrin-A5$^{-/-}$ eye. (**A**, **B**) Representative pictures of the retrolental mass seen in an ephrin-A5$^{-/-}$ eye at P7 and P21. Sections are labeled with TRP-1 to delineate cells encompassing the mass. *Scale bar*: 200 μm. (**C**) Quantification of the relative volume of the retrolental mass at P7 and P21. The size of the fibroblastic mass is significantly larger at P21 than at P7 ($P < 0.05$, $n = 4$ per group). (**D**, **E**) BrdU incorporation and PCNA staining of the retrolental tissue in the ephrin-A5$^{-/-}$ eye at P7, indicating cell division occurring in postnatal stages. *Scale bar*: 200 μm. (**F**–**I**) BrdU incorporation and labeling at various developmental periods in the WT and ephrin-A5$^{-/-}$ eye. Pregnant mice were injected with BrdU 2 hours before euthanasia, and embryos subsequently were fixed. *Scale bar*: 200 μm. (**J**) Quantification of the percentage BrdU positive cells in the retrolental mass during development. A greater percentage of BrdU positive cells is observed in the ephrin-A5 null eye at E14 and E16, though this effect is significant only at E16 ($P > 0.05$ at E14, $P < 0.05$ at E16, $n = 4$ per group).

postnatal stages (Fig. 8E), indicating continued growth of this aberrant tissue in the ephrin-A5$^{-/-}$ eye in postnatal stages.

Based on these results, we next determined whether the persistence of the primary vitreous was due to changes in cell division within the primary vitreous during embryonic development (Figs. 8F–J). Embryos at E14 and E16 were labeled using BrdU, and staining was compared between wild-type and ephrin-A5$^{-/-}$ animals. Mice at their respective stages were injected with BrdU two hours before being euthanized, after which embryos were dissected and fixed for cryosectioning. At E14, cells of the primary vitreous in wild-type (Fig. 8F) and ephrin-A5$^{-/-}$ (Fig. 8H) embryos displayed a large percentage of BrdU positive cells with no statistical difference observed between the groups (Fig. 8J, wild-type = 19.99% ± 3.99%, ephrin-A5$^{-/-}$ = 24.92% ± 3.32%, $P > 0.05$, $n = 4$), suggesting that the increased number of cells in the mutant vitreous is due to recruitment rather than increased mitosis. However, by E16, while the proliferation rate was decreased in wild-type (Fig. 8G) and ephrin-A5$^{-/-}$ (Fig. 8I) animals compared to at E14, the percentage of BrdU positive cells of the ephrin-A5$^{-/-}$ embryos was higher than that of wild-type animals (Fig. 8J, wild-type = 8.6% ± 2.58%, ephrin-A5$^{-/-}$ = 15.4% ± 1.84%, $P < 0.05$, $n = 4$). Wild-type and ephrin-A5$^{-/-}$ primary vitreous tissues also were analyzed for apoptosis using an antibody against cleaved caspase-3 (Supplementary Fig. S4). Wild-type and ephrin-A5$^{-/-}$ primary vitreous tissues at E14 and E16 showed signs of cells undergoing apoptosis (cleaved caspase-3) (Supplementary Figs. S4A, S4B), but the percentage of cleaved caspase-3–positive cells was not significantly different between the two groups (Supplementary Fig. S4C). Altogether, these data indicated that the increased retrolental cell mass size is due to excess cell recruitment and not increased mitosis or decreased apoptosis during early eye morphogenesis before E14. However, after E16, cell growth in wild type retrolental mass was significantly reduced, while the mass continued to grow in the ephrin-A5$^{-/-}$ eye.

Discussion

In this current study, we reported for the first time to our knowledge that mice lacking the Eph receptor ligand ephrin-A5 develop the ocular pathology PHPV, more recently termed PFV. Postnatal ephrin-A5$^{-/-}$ mice develop a large pigmented retrolental mass that persists throughout the lifetime of the animal. The hyperplastic mass is derived from primary vitreous cells that have failed to regress and consists of neural crest-derived cells encompassing vascular structures. The EphA receptor expression is observed throughout the retrolental mass, while ephrin-A5 expression was notably absent within the primary vitreous in wild-type tissues. However, ephrin-A5 expression was present at high levels in the frontal eye

segment through which neural crest and mesenchymal cells destined for the primary vitreous migrate into the retrolental space. Additionally, the cells within the persistent retrolental structure are mitotically active at postnatal stages in ephrin-A5$^{-/-}$ animals.

The Complex Relationship Between PHPV and Primary Vitreous Regression

The conditions of PHPV and PFV have been defined classically as diseases resulting from the failed regression of intraocular vasculature.[4] However, the cellular mechanisms underlying the primary vitreous regression defect remain poorly understood. In the past, much of the focus on the disease has been on the vascular component, specifically in the mechanisms underlying the regression of the hyaloid vasculature. In mice, hyaloid regression occurs in the first few weeks of postnatal development, during which time retinal vasculature begins to form.[5] Hyaloid development is dependent on several factors, including VEGF,[22,23] which is expressed in the lens during early ocular development and is required for the maintenance of the early vascular network.[5,61–63] The degradation of this structure is mediated by apoptotic[48,64,65] and autophagic mechanisms,[66] and responds to levels of oxygen.[67–69]

However, while much of the focus in past research has been on vascular regression, the complex etiology of PHPV/PFV leaves much to be understood. The primary vitreous, from which the hyaloid network forms, contains cells of neural crest and mesodermal origins.[1,2,5] Additionally, reported incidences of PHPV/PFV in human cases and animal models also have pointed to a complex pathology that consists of being more than simply a failure of vascular regression. In humans, the presence of pigmented cells within the retrolental mass has been described previously.[12] Vitreous cysts, a PHPV-like condition in which aberrant masses are formed within the vitreous humor, also have been reported to be composed of pigmented cells and hyaloid vasculature,[9–11] and in some of these cases, have been hypothesized to be remnants of the primary vitreous.[10]

Also, PHPV has been studied extensively and observed in other animal species in which pigmentation of the retrolental mass has been a defining characteristic. In dog breeds that have high prevalence of this condition, pigmentation of the fibrovascular mass is a common characteristic of the disorder, with the extent of pigmentation being an indicator of the severity of the condition.[8,13–15,70] Several PHPV mouse models also have reported pigmentation of the retrolental mass at postnatal periods.[16,17,21] Additionally, other cell types, including astrocytes, have been found to have a role in PHPV, as their deficiency accelerates hyaloid regression[71] and their interaction with the hyaloid vasculature is thought to inhibit regression by macrophages.[72,73]

The persistent mass observed in ephrin-A5$^{-/-}$ mice further verifies the complexity of the primary vitreous degeneration process containing several aspects that include, but are not limited to, hyaloid vessel regression.[48,65] The presence of pigmented and vascular structures in the retrolental mass along with the continued degeneration of the TVL in ephrin-A5$^{-/-}$ mice indicates that ephrin-A5 is important in the overall regression of the primary vitreous and not the hyaloid vasculature. Indeed, hyaloid vessels in areas not encapsulated by the pigmented cell mass, in particular the TVL, regress over time at similar rates between the wild-type and ephrin-A5$^{-/-}$ eyes. While the retrolental mass observed in ephrin-A5$^{-/-}$ eyes also contains extensive vascular structures, the most prominent feature has been the presence of pigmented cells of neural crest origin surrounding the vasculature. In this sense, the name persistent hyperplastic primary vitreous may be more accurate than persistent fetal vasculature, at least in the context of ephrin-A5$^{-/-}$ mice, since the aberrant structure consists of vascular and pigmented cells.

Pigmented Structures in Primary Vitreous Are of Neural Crest Origin

Accumulation of pigmented cells have been documented previously in PHPV cases within humans[12] and dogs, as well as in conditions related to PHPV, such as vitreal cysts. In addition, several mouse models of the disease also have reported the presence of postnatal pigmentation within the retrolental mass.[16,17] One of the underlying questions in determining the mechanisms underlying primary vitreous regression has been in understanding the origin of these pigmented cells. Melanocytes arise from two distinct cellular populations: the neural crest or the retinal pigmented epithelium.[51] It has been proposed previously that PHPV is a result of the accumulation of RPE cells around hyaloid vasculature.[12,17]

Similarly, we have found the pigmented cells surrounding the vasculature in the ephrin-A5$^{-/-}$ mice. However, several lines of evidence, including the difference in onset of pigmentation in the primary vitreous versus the RPE layer and the neural crest marker labeling of the primary vitreous cells, indicate the origin of these pigmented cells in our model to be of neural crest origin and not from the RPE. We believe primary vitreous cells of neural crest origin that have failed to regress in the ephrin-A5$^{-/-}$ eye produce melanin in postnatal periods and continue to proliferate throughout the lifetime of the animal. Whether human PHPV also contains neural crest cells is yet to be determined.

The Role of Ephrin-A5 and EphA Receptors in Primary Vitreous Regression

While ephrin-A5 has a key role in primary vitreous regression, the mechanisms underlying the persistence of the retrolental cell mass in ephrin-A5$^{-/-}$ eyes remain to be resolved. The Eph family has been identified previously in having important roles in vascular[56,74–78] and neural crest[79–82] biology. In this study we showed that the ephrin-A5$^{-/-}$ primary vitreous has an increased number of mesoderm- and neural crest-derived cells as early as E11. We also have observed high levels of ephrin-A5 in the frontal segment of the developing eye, including the cornea, through which these cells migrate into the primary vitreous. One possibility is that ephrin-A5 inhibits the migration of cells recruited into the primary vitreous. Since melanocytes are fated relatively late during neural crest migration,[83,84] it also is possible that the high levels of ephrin-A5 expressed in the corneal epithelium prevent melanocyte-fated neural crest cell migration into the vitreous. The persistence of melanocytes in the ephrin-A5$^{-/-}$ primary vitreous may reflect the fact that the primary vitreous regression mechanism lacks the ability to remove these melanocyte-fated cells, which migrate in abnormally in the absence of ephrin-A5. These observations suggest a novel mechanism that may contribute to PHPV development.

This mechanism is consistent with the observation that no or very low levels of ephrin-A5 have been detected in the wild-type primary vitreous. However, since several Eph receptors have been found within the retrolental cell mass, we cannot exclude other potential mechanisms by which ephrin-A5 may regulate hyaloid regression. Several previous studies have identified A-classed ephrins to be capable of being cleaved while retaining some functional activity.[30–32] Our current study identified high levels of ephrin-A ligands throughout other developing ocular tissues, including the ciliary body and lens.

Investigative Ophthalmology & Visual Science

Therefore, ephrin-A5 expressed in these tissues may be released into the primary vitreous and directly influence the regression of the primary vitreous.

Ephrin-A5 also may be regulating the release of other factors that would normally affect primary vitreous regression. Diffusible factors within the lens, such as VEGF, have been found previously to regulate hyaloid vessel formation and regression,[85,86] and platelet-derived growth factor (PDGF) signaling has been implicated in primary vitreous regression.[87] The high levels of ephrin-A5 in surrounding ocular tissues, therefore, may be negatively regulating the release of mitotic factors, such as VEGF or PDGF, resulting in the regression of the primary vitreous tissue.

A final possibility is that ephrin-A5 within the primary vitreous is expressed at low levels during the regression process. We detected ephrin-A ligand expression using an EphA5-AP binding method that showed high levels of specificity. However, this staining method may lack the sensitivity to detect low concentrations of ephrin-A5 expression within the primary vitreous tissue undergoing degradation. Further studies are required to elucidate the role of ephrin-A5 during this degeneration process.

Acknowledgments

The authors thank Jonas Frisen (Karolinska Institute, Stockholm, Sweden) for providing the ephrin-A5$^{-/-}$ mice; and Janet Alder and Smita Thakker-Varia (Robert Wood Johnson Medical School, University of Medicine and Dentistry of New Jersey, Piscataway, NJ) for their support with the RT-PCR experiment.

Supported by Grants R01EY019012 from the National Eye Institute and F31AG032806 from the National Institute on Aging.

Disclosure: **A.I. Son**, None; **M. Sheleg**, None; **M.A. Cooper**, None; **Y. Sun**, None; **N.J. Kleiman**, None; **R. Zhou**, None

References

1. Gage PJ, Rhoades W, Prucka SK, Hjalt T. Fate maps of neural crest and mesoderm in the mammalian eye. *Invest Ophthalmol Vis Sci*. 2005;46:4200–4208.
2. Ittner LM, Wurdak H, Schwerdtfeger K, et al. Compound developmental eye disorders following inactivation of TGFbeta signaling in neural-crest stem cells. *J Biol*. 2005;4:11.
3. Ito M, Yoshioka M. Regression of the hyaloid vessels and pupillary membrane of the mouse. *Anat Embryol (Berl)*. 1999;200:403–411.
4. Goldberg MF. Persistent fetal vasculature (PFV): an integrated interpretation of signs and symptoms associated with persistent hyperplastic primary vitreous (PHPV). LIV Edward Jackson Memorial Lecture. *Am J Ophthalmol*. 1997;124:587–626.
5. Saint-Geniez M, D'Amore PA. Development and pathology of the hyaloid, choroidal and retinal vasculature. *Int J Dev Biol*. 2004;48:1045–1058.
6. Pollard ZF. Persistent hyperplastic primary vitreous: diagnosis, treatment and results. *Trans Am Ophthalmol Soc*. 1997;95:487–549.
7. Shastry BS. Persistent hyperplastic primary vitreous: congenital malformation of the eye. *Clin Experiment Ophthalmol*. 2009;37:884–890.
8. Leon A. Diseases of the vitreous in the dog and cat. *J Small Anim Pract*. 1988;29:448–461.
9. Nork TM, Millecchia LL. Treatment and histopathology of a congenital vitreous cyst. *Ophthalmology*. 1998;105:825–830.
10. Cruciani F, Santino G, Salandri AG. Monolateral idiopathic cyst of the vitreous. *Acta Ophthalmol Scand*. 1999;77:601–603.
11. Brue C, Mariotti C, De Franco E, De Franco N, Giovannini A. Pigmented free-floating posterior vitreous cyst. *Case Rep Ophthalmol Med*. 2012;2012:470289.
12. Haddad R, Font RL, Reeser F. Persistent hyperplastic primary vitreous. A clinicopathologic study of 62 cases and review of the literature. *Surv Ophthalmol*. 1978;23:123–134.
13. Curtis R, Barnett KC, Leon A. Persistent hyperplastic primary vitreous in the Staffordshire bull terrier. *Vet Rec*. 1984;115:385.
14. Stades FC. Persistent hyperplastic tunica vasculosa lentis and persistent hyperplastic primary vitreous (PHTVL/PHPV) in 90 closely reltaed Doberman Pinschers: clinical aspects. *J Am Animal Hosp Assoc*. 1980;16:739–751.
15. Stades FC, Boeve MH, van den Brom WE, van der Linde-Sipman JS. The incidence of PHTVL/PHPV in Doberman and the results of breeding rules. *Vet Quart*. 1991;13:24–29.
16. McKeller RN, Fowler JL, Cunningham JJ, et al. The Arf tumor suppressor gene promotes hyaloid vascular regression during mouse eye development. *Proc Natl Acad Sci U S A*. 2002;99:3848–3853.
17. Martin AC, Thornton JD, Liu J, et al. Pathogenesis of persistent hyperplastic primary vitreous in mice lacking the arf tumor suppressor gene. *Invest Ophthalmol Vis Sci*. 2004;45:3387–3396.
18. Thornton JD, Swanson DJ, Mary MN, et al. Persistent hyperplastic primary vitreous due to somatic mosaic deletion of the arf tumor suppressor. *Invest Ophthalmol Vis Sci*. 2007;48:491–499.
19. Freeman-Anderson NE, Zheng Y, McCalla-Martin AC, et al. Expression of the Arf tumor suppressor gene is controlled by Tgfbeta2 during development. *Development*. 2009;136:2081–2089.
20. Reichel MB, Ali RR, D'Esposito F, et al. High frequency of persistent hyperplastic primary vitreous and cataracts in p53-deficient mice. *Cell Death Differ*. 1998;5:156–162.
21. Zhang J, Fuhrmann S, Vetter ML. A nonautonomous role for retinal frizzled-5 in regulating hyaloid vitreous vasculature development. *Invest Ophthalmol Vis Sci*. 2008;49:5561–5567.
22. Rutland CS, Mitchell CA, Nasir M, Konerding MA, Drexler HC. Microphthalmia, persistent hyperplastic hyaloid vasculature and lens anomalies following overexpression of VEGF-A188 from the alphaA-crystallin promoter. *Mol Vis*. 2007;13:47–56.
23. Mitchell CA, Rutland CS, Walker M, et al. Unique vascular phenotypes following over-expression of individual VEGFA isoforms from the developing lens. *Angiogenesis*. 2006;9:209–224.
24. Pasquale EB. Eph receptors and ephrins in cancer: bidirectional signalling and beyond. *Nat Rev Cancer*. 2010;10:165–180.
25. Himanen JP, Chumley MJ, Lackmann M, et al. Repelling class discrimination: ephrin-A5 binds to and activates EphB2 receptor signaling. *Nat Neurosci*. 2004;7:501–509.
26. Pasquale EB. Eph receptor signalling casts a wide net on cell behaviour. *Nat Rev Mol Cell Biol*. 2005;6:462–475.
27. Klein R. Bidirectional modulation of synaptic functions by Eph/ephrin signaling. *Nat Neurosci*. 2009;12:15–20.
28. Daar IO. Non-SH2/PDZ reverse signaling by ephrins. *Semin Cell Dev Biol*. 2012;23:65–74.
29. Xu NJ, Henkemeyer M. Ephrin reverse signaling in axon guidance and synaptogenesis. *Semin Cell Dev Biol*. 2012;23:58–64.
30. Hattori M, Osterfield M, Flanagan JG. Regulated cleavage of a contact-mediated axon repellent. *Science*. 2000;289:1360–1365.
31. Wykosky J, Palma E, Gibo DM, Ringler S, Turner CP, Debinski W. Soluble monomeric EphrinA1 is released from tumor cells and is a functional ligand for the EphA2 receptor. *Oncogene*. 2008;27:7260–7273.

32. Alford S, Watson-Hurthig A, Scott N, et al. Soluble ephrin a1 is necessary for the growth of HeLa and SK-BR3 cells. *Cancer Cell Int*. 2010;10:41.
33. Cooper MA, Son AI, Komlos D, Sun Y, Kleiman NJ, Zhou R. Loss of ephrin-A5 function disrupts lens fiber cell packing and leads to cataract. *Proc Natl Acad Sci U S A*. 2008;105:16620–16625.
34. Jun G, Guo H, Klein BE, et al. EPHA2 is associated with age-related cortical cataract in mice and humans. *PLoS Genet*. 2009;5:e1000584.
35. Feldheim DA, Kim YI, Bergemann AD, Frisen J, Barbacid M, Flanagan JG. Genetic analysis of ephrin-A2 and ephrin-A5 shows their requirement in multiple aspects of retinocollicular mapping. *Neuron*. 2000;25:563–574.
36. Sheleg M, Yochum CL, Wagner GC, Zhou R, Richardson JR. Ephrin-A5 deficiency alters sensorimotor and monoaminergic development. *Behav Brain Res*. 2012;236C:139–147.
37. Akaneya Y, Sohya K, Kitamura A, et al. Ephrin-A5 and EphA5 interaction induces synaptogenesis during early hippocampal development. *PLoS One*. 2010;5:e12486.
38. Cooper MA, Crockett DP, Nowakowski RS, Gale NW, Zhou R. Distribution of EphA5 receptor protein in the developing and adult mouse nervous system. *J Comp Neurol*. 2009;514:310–328.
39. Gao PP, Zhang JH, Yokoyama M, et al. Regulation of topographic projection in the brain: Elf-1 in the hippocamposeptal system. *Proc Natl Acad Sci U S A*. 1996;93:11161–11166.
40. Flanagan JG. Neural map specification by gradients. *Curr Opin Neurobiol*. 2006;16:59–66.
41. Cheng C, Gong X. Diverse roles of Eph/ephrin signaling in the mouse lens. *PLoS One*. 2011;6:e28147.
42. Son AI, Park JE, Zhou R. The role of Eph receptors in lens function and disease. *Science China Life Sci*. 2012;55:434–443.
43. Son AI, Cooper MA, Sheleg M, Sun Y, Kleiman NJ, Zhou R. Further analysis of the lens of ephrin-A5-/- mice: development of postnatal defects. *Mol Vis*. 2013;19:254–266.
44. Frisen J, Yates PA, McLaughlin T, Friedman GC, O'Leary DD, Barbacid M. Ephrin-A5 (AL-1/RAGS) is essential for proper retinal axon guidance and topographic mapping in the mammalian visual system. *Neuron*. 1998;20:235–243.
45. van Eyll JM, Passante L, Pierreux CE, Lemaigre FP, Vanderhaeghen P, Rousseau GG. Eph receptors and their ephrin ligands are expressed in developing mouse pancreas. *Gene Expr Patterns*. 2006;6:353–359.
46. Zhang JH, Cerretti DP, Yu T, Flanagan JG, Zhou R. Detection of ligands in regions anatomically connected to neurons expressing the Eph receptor Bsk: potential roles in neuron-target interaction. *J Neurosci*. 1996;16:7182–7192.
47. Washburn CP, Cooper MA, Zhou R. Expression of the tyrosine kinase receptor EphA5 and its ligand ephrin-A5 during mouse spinal cord development. *Neurosci Bull*. 2007;23:249–255.
48. Lobov IB, Rao S, Carroll TJ, et al. WNT7b mediates macrophage-induced programmed cell death in patterning of the vasculature. *Nature*. 2005;437:417–421.
49. Bullock JD. Developmental vitreous cysts. *Arch Ophthalmol*. 1974;91:83–84.
50. Orellana J, O'Malley RE, McPherson AR, Font RL. Pigmented free-floating vitreous cysts in two young adults. Electron microscopic observations. *Ophthalmology*. 1985;92:297–302.
51. Goding CR. Melanocytes: the new black. *Int J Biochem Cell Biol*. 2007;39:275–279.
52. Hu DN, Simon JD, Sarna T. Role of ocular melanin in ophthalmic physiology and pathology. *Photochem Photobiol*. 2008;84:639–644.
53. Mitchell PJ, Timmons PM, Hebert JM, Rigby PW, Tjian R. Transcription factor AP-2 is expressed in neural crest cell lineages during mouse embryogenesis. *Genes Dev*. 1991;5:105–119.
54. Marcus RC, Matthews GA, Gale NW, Yancopoulos GD, Mason CA. Axon guidance in the mouse optic chiasm: retinal neurite inhibition by ephrin "A"-expressing hypothalamic cells in vitro. *Dev Biol*. 2000;221:132–147.
55. Helbling PM, Tran CT, Brandli AW. Requirement for EphA receptor signaling in the segregation of Xenopus third and fourth arch neural crest cells. *Mech Dev*. 1998;78:63–79.
56. Chen J, Hicks D, Brantley-Sieders D, et al. Inhibition of retinal neovascularization by soluble EphA2 receptor. *Exp Eye Res*. 2006;82:664–673.
57. Brantley-Sieders DM, Caughron J, Hicks D, Pozzi A, Ruiz JC, Chen J. EphA2 receptor tyrosine kinase regulates endothelial cell migration and vascular assembly through phosphoinositide 3-kinase-mediated Rac1 GTPase activation. *J Cell Sci*. 2004;117:2037–2049.
58. Cheng N, Brantley D, Fang WB, et al. Inhibition of VEGF-dependent multistage carcinogenesis by soluble EphA receptors. *Neoplasia*. 2003;5:445–456.
59. Cheng N, Brantley DM, Liu H, et al. Blockade of EphA receptor tyrosine kinase activation inhibits vascular endothelial cell growth factor-induced angiogenesis. *Mol Cancer Res*. 2002;1:2–11.
60. Ogawa K, Pasqualini R, Lindberg RA, Kain R, Freeman AL, Pasquale EB. The ephrin-A1 ligand and its receptor, EphA2, are expressed during tumor neovascularization. *Oncogene*. 2000;19:6043–6052.
61. Gogat K, Le Gat L, Van Den Berghe L, et al. VEGF and KDR gene expression during human embryonic and fetal eye development. *Invest Ophthalmol Vis Sci*. 2004;45:7–14.
62. Mitchell CA, Risau W, Drexler HC. Regression of vessels in the tunica vasculosa lentis is initiated by coordinated endothelial apoptosis: a role for vascular endothelial growth factor as a survival factor for endothelium. *Dev Dyn*. 1998;213:322–333.
63. Shui YB, Wang X, Hu JS, et al. Vascular endothelial growth factor expression and signaling in the lens. *Invest Ophthalmol Vis Sci*. 2003;44:3911–3919.
64. Lang RA, Bishop JM. Macrophages are required for cell death and tissue remodeling in the developing mouse eye. *Cell*. 1993;74:453–462.
65. Kato M, Patel MS, Levasseur R, et al. Cbfa1-independent decrease in osteoblast proliferation, osteopenia, and persistent embryonic eye vascularization in mice deficient in Lrp5, a Wnt coreceptor. *J Cell Biol*. 2002;157:303–314.
66. Kim JH, Yu YS, Mun JY, Kim KW. Autophagy-induced regression of hyaloid vessels in early ocular development. *Autophagy*. 2010;6:922–928.
67. Bischoff PM, Wajer SD, Flower RW. Scanning electron microscopic studies of the hyaloid vascular system in newborn mice exposed to O2 and CO2. *Graefes Arch Clin Exp Ophthalmol*. 1983;220:257–263.
68. Patz A, Eastham A, Higginbotham DH, Kleh T. Oxygen studies in retrolental fibroplasia. II. The production of the microscopic changes of retrolental fibroplasia in experimental animals. *Am J Ophthalmol*. 1953;36:1511–1522.
69. Gyllensten LJ, Hellstrom BE. Experimental approach to the pathogenesis of retrolental fibroplasia. I. Changes of the eye induced by exposure of newborn mice to concentrated oxygen. *Acta Paed Suppl*. 1954;43:131–148.
70. Boeve MH, van der Linde-Sipman JS, Stades FC, Vrensen GF. Early morphogenesis of persistent hyperplastic tunica vasculosa lentis and primary vitreous. A transmission electron microscopic study. *Invest Ophthalmol Vis Sci*. 1990;31:1886–1894.
71. Kurihara T, Westenskow PD, Krohne TU, Aguilar E, Johnson RS, Friedlander M. Astrocyte pVHL and HIF-alpha isoforms are

Investigative Ophthalmology & Visual Science

required for embryonic-to-adult vascular transition in the eye. *J Cell Biol*. 2011;195:689–701.

72. Zhang C, Asnaghi L, Gongora C, et al. A developmental defect in astrocytes inhibits programmed regression of the hyaloid vasculature in the mammalian eye. *Eur J Cell Biol*. 2011;90:440–448.
73. Zhang C, Gehlbach P, Gongora C, et al. A potential role for beta- and gamma-crystallins in the vascular remodeling of the eye. *Dev Dyn*. 2005;234:36–47.
74. Wang HU, Chen ZF, Anderson DJ. Molecular distinction and angiogenic interaction between embryonic arteries and veins revealed by ephrin-B2 and its receptor Eph-B4. *Cell*. 1998;93:741–753.
75. Gerety SS, Wang HU, Chen ZF, Anderson DJ. Symmetrical mutant phenotypes of the receptor EphB4 and its specific transmembrane ligand ephrin-B2 in cardiovascular development. *Mol Cell*. 1999;4:403–414.
76. Foo SS, Turner CJ, Adams S, et al. Ephrin-B2 controls cell motility and adhesion during blood-vessel-wall assembly. *Cell*. 2006;124:161–173.
77. Semela D, Das A, Langer D, Kang N, Leof E, Shah V. Platelet-derived growth factor signaling through ephrin-b2 regulates hepatic vascular structure and function. *Gastroenterology*. 2008;135:671–679.
78. Ojima T, Takagi H, Suzuma K, et al. EphrinA1 inhibits vascular endothelial growth factor-induced intracellular signaling and suppresses retinal neovascularization and blood-retinal barrier breakdown. *Am J Pathol*. 2006;168:331–339.
79. Wang HU, Anderson DJ. Eph family transmembrane ligands can mediate repulsive guidance of trunk neural crest migration and motor axon outgrowth. *Neuron*. 1997;18:383–396.
80. Krull CE, Lansford R, Gale NW, et al. Interactions of Eph-related receptors and ligands confer rostrocaudal pattern to trunk neural crest migration. *Curr Biol*. 1997;7:571–580.
81. Kasemeier-Kulesa JC, Bradley R, Pasquale EB, Lefcort F, Kulesa PM. Eph/ephrins and N-cadherin coordinate to control the pattern of sympathetic ganglia. *Development*. 2006;133:4839–4847.
82. Santiago A, Erickson CA. Ephrin-B ligands play a dual role in the control of neural crest cell migration. *Development*. 2002;129:3621–3632.
83. Harris ML, Erickson CA. Lineage specification in neural crest cell pathfinding. *Dev Dyn*. 2007;236:1–19.
84. Dupin E, Le Douarin NM. Development of melanocyte precursors from the vertebrate neural crest. *Oncogene*. 2003;22:3016–3023.
85. Garcia CM, Shui YB, Kamath M, et al. The function of VEGF-A in lens development: formation of the hyaloid capillary network and protection against transient nuclear cataracts. *Exp Eye Res*. 2009;88:270–276.
86. Beebe DC. Maintaining transparency: a review of the developmental physiology and pathophysiology of two avascular tissues. *Semin Cell Dev Biol*. 2008;19:125–133.
87. Silva RL, Thornton JD, Martin AC, et al. Arf-dependent regulation of Pdgf signaling in perivascular cells in the developing mouse eye. *EMBO J*. 2005;24:2803–2814.

Investigative Ophthalmology & Visual Science